HHS Public Access

Author manuscript

J Cell Physiol. Author manuscript; available in PMC 2019 February 01.

Published in final edited form as:

J Cell Physiol. 2018 February ; 233(2): 1585–1600. doi:10.1002/jcp.26062.

High fat diet attenuates hyperglycemia, body composition changes, and bone loss in male streptozotocin-induced type 1 diabetic mice

Adriana Lelis Carvalho[1,2], **Victoria E. DeMambro**[1], **Anyonya R. Guntur**[1], **Phuong Le**[1], **Kenichi Nagano**[3], **Roland Baron**[3], **Francisco José Albuquerque de Paula**[2], and **Katherine J. Motyl**[1,4,*]

[1]Center for Clinical and Translational Research, Maine Medical Center Research Institute, Scarborough, Maine 04074.

[2]Internal Medicine Department, Ribeirão Preto Medical School, University of São Paulo, Brazil

[3]Department of Oral Medicine, Infection and Immunity, Harvard School of Dental Medicine, Harvard University, Boston, Massachusetts 02115

[4]Center for Molecular Medicine, Maine Medical Center Research Institute, Scarborough, Maine 04074

Abstract

There is a growing and alarming prevalence of obesity and the metabolic syndrome in type I diabetic patients (T1DM), particularly in adolescence. In general, low bone mass, higher fracture risk and increased marrow adipose tissue (MAT) are features of diabetic osteopathy in insulin deficient subjects. On the other hand, type 2 diabetes (T2DM) is associated with normal or high bone mass, a greater risk of peripheral fractures and no change in MAT. Therefore, we sought to determine the effect of weight gain on bone turnover in insulin deficient mice. We evaluated the impact of a 6-week high-fat (HFD) rich in medium chain fatty acids or low-fat diet (LFD) on bone mass and MAT in a streptozotocin (STZ)-induced model using male C57BL/6J mice at 8 weeks of age. Dietary intervention was initiated after diabetes confirmation. At the endpoint, lower non-fasting glucose levels were observed in diabetic mice fed with high fat diet compared to diabetic mice fed the low fat diet (STZ-LFD). Compared to euglycemic controls, the STZ-LFD had marked polydipsia and polyphagia, as well as reduced lean mass, fat mass and bone parameters. Interestingly, STZ-HFD mice had higher bone mass, namely less cortical bone loss and more trabecular bone than STZ-LFD. Thus, we found that a HFD, rich in medium chain fatty acids, protects against bone loss in a T1DM mouse model. Whether this may also translate to T1DM patients who are overweight or obese in respect to maintenance of bone mass remains to be determined through longitudinal studies.

[*]*Address all correspondence and requests for reprints to:* Dr. Katherine J. Motyl, Maine Medical Center Research Institute, 81 Research Drive, Scarborough, ME 04074–7205. motylk@mmc.org.

Disclosure Statement: The authors have nothing to disclose.

Keywords

Type 1 Diabetes Mellitus; Bone Mass; High Fat Diet; Bone Marrow Adipose Tissue

INTRODUCTION

Type 1 diabetes mellitus (T1DM) is associated with low bone mineral density (BMD) and increased fracture risk (Tuominen et al., 1999). Several studies have shown that bone loss in T1DM occurs because of reduced bone formation, while the effects on bone resorption are less clear (Hough et al., 2016; McCabe, 2007). There are several characteristics of T1DM that may have a significant impact on bone, such as hypoinsulinemia and high glucose levels (de Paula et al., 2010; Hough et al., 2016). Due to the positive effects of insulin and IGF-1 on bone formation, decreased insulin signaling has been considered as one of the most critical factors in the pathogenesis of T1DM-bone loss (Kawai and Rosen, 2010). However, mice with an osteoblast-specific knockout of insulin receptor only have a mild low bone mass phenotype in adult mice (Fulzele et al., 2010). Moreover, adult mice with a global knockout of insulin receptor, made normoglycemic by knock in of the human insulin receptor in liver, brain and pancreas, also have a normal bone phenotype (Irwin et al., 2006). Hyperglycemia, on the other hand, can impair osteoblast differentiation in culture and elevated advanced glycation end products (AGES) have been associated with fractures in patients with T1DM (Botolin and McCabe, 2006; Neumann et al., 2014). Moreover, high glucose levels have also been positively linked to greater marrow adiposity in non-diabetic women (de Paula et al., 2015b).

T1DM critically impacts whole body energy economy, leading to weight loss due to increased proteolysis and lipolysis. Bone catabolism is a well-known complication of weight loss and occurs because of an array of factors, including decreased mechanical loading and nutritional and hormonal changes (Basso et al., 2005; Cao, 2011; Devlin and Rosen, 2015; Komori, 2015). In conditions of chronic (i.e., anorexia nervosa) as well as acute weight loss (i.e., bariatric surgery) a negative remodeling balance is a well-documented occurrence (Bredella et al., 2009; Devlin et al., 2010; Reid, 2010). Low body weight is a frequent clinical manifestation during the onset of T1DM (Association, 2009). However, recent publications have pointed out the alarming rise in obesity in T1DM individuals (Conway et al., 2010; Liu et al., 2010). In one prospective study, 18 years of follow-up showed that 20% of T1DM subjects enrolled in the study had gained at least 5 kg/m^2 while only 7% had lost at least 2 kg/m^2. The number of overweight individuals increased in 47% during the period of the follow-up (Conway et al., 2010). As a consequence, there has been a growing prevalence of abdominal obesity, insulin resistance and arterial hypertension among T1DM children and adults that paradoxically were previously considered to be pathognomonic of T2DM (da Costa et al., 2016; Merger et al., 2016; Polsky and Ellis, 2015). The increase in metabolic syndrome characteristics in T1DM patients appear to be an important risk factor for the development of macrovascular and microvascular comorbidities such as cardiovascular diseases, diabetic foot syndrome, nephropathy, and retinopathy, independently of glucose control (Merger et al., 2016). However, the effect of high body weight or obesity on bone mass and bone turnover in T1DM is still unknown.

Obesity is characterized by excessive body fat accumulation and despite higher or normal BMD, fracture risk is also increased in obese subjects (Paula and Rosen, 2010). The intake of a diet rich in saturated fats is well-documented to be associated with greater body fat content, insulin resistance (Petro et al., 2004) and also with reduction of BMD (Corwin et al., 2006; Macri et al., 2012). Hence, we sought to determine the impact of weight gain on bone mass in streptozotocin (STZ)-induced T1DM mice. We hypothesized that high fat feeding would not be able to counteract classical type 1 diabetic bone loss and may in fact make it worse. For this, we submitted eight-week-old male T1DM and control mice to 6-week high saturated fat diet (HFD) rich in medium chain fatty acid (MCFA) or low fat diet (LFD). In brief, although HFD is generally deleterious to bone, we found that HFD actually attenuated trabecular and cortical bone loss from STZ-induced diabetes, without significantly affecting insulin levels. Blood glucose was lower and body weights were higher in HFD-fed STZ mice compared to LFD-fed STZ mice, suggesting glycemic control and/or body weight played a protective role in T1DM bone disease.

MATERIALS AND METHODS

The study protocol was approved by the Institutional Animal Care and Use Committees (IACUC) of the Maine Medical Center Research Institute (MMCRI). All animals were maintained on a 14-h light and 10-h dark cycle in a barrier animal facility at MMCRI. Mice were given water and food (see below for detailed description of diets) *ad libitum* and housed 3–4 per cage. All mice had body weight measured weekly during the experiment.

Diabetes Induction and Dietary Intervention

Six-week-old male C57BL/6J mice were obtained from the Jackson Laboratory (Bar Harbor, ME). At 8 weeks of age, they were administered 5 daily intraperitoneal (IP) injections of streptozotocin (STZ) (50 mg/kg body weight in 0.1 M citrate buffer pH 4.5; Sigma-Aldrich) to induce diabetes or vehicle (0.1 M citrate buffer pH 4.5) injections. All mice received standard diet (2018 Teklad Global 18% Protein Rodent Diet, Harlan Laboratories) until diabetes confirmation. Twelve days after the first injection, non-fasting blood glucose levels were assessed using an Accu-Check Compact® glucometer (Roche Diagnostics, Indianapolis, IN). The blood glucose cut-off was 16.7 mmol/L (300 mg/dL) for including animals in STZ groups. Non-fasting glucose levels were also checked at the endpoint of the study. After diabetes confirmation, mice were divided into four different groups for 6 weeks of diet intervention (Research Diets Inc., New Brunswick, NJ, Supplemental Table I):

I. **Control Low Fat Diet (CON-LFD):** mice injected with vehicle solution (n=11), then fed with custom formulated low fat diet (Research Diets D15022202) containing 11% Kcal from fat, and 73% Kcal from carbohydrate comprised of corn starch and an amount of sucrose matched with HFD.

II. **Control High Fat Diet (CON-HFD):** mice injected with vehicle solution (n=11), then fed with a high fat diet (Research Diets D12331i) containing 58% Kcal from hydrogenated coconut oil, and 26% Kcal from sucrose.

III. **STZ Low Fat Diet (STZ-LFD):** mice injected with STZ solution (n=9), then fed with custom formulated 11% kcal from fat diet (Research Diets D15022202).

IV. **STZ High Fat Diet (STZ-HFD):** mice injected with STZ solution (n=14), then fed with 58% Kcal from fat diet (Research Diets D12331i).

Serum Assays

Serum insulin levels were measured using a commercially available kit from Crystal Chem Inc. (Downers Grove, IL), according to the manufacturer's instructions. The assay sensitivity was 0.05 ng/mL. The intra- and inter-assay variability was ≤ 10 ng/mL. Serum P1NP and CTx levels were measured using commercially available kits from IDS (Gaithersburg, MD) according to the manufacturer's instructions. The assay sensitivities were 0.7 and 2 ng/mL for P1NP and CTx, respectively. The intra-assay variations were 6.3 and 6.9%, and the inter-assay variations were 8.5 and 12% respectively, for both assays. All measurements were performed in duplicate. β-hydroxybutyrate was measured with an assay kit (MAK041, Sigma) according to the manufacturer's instructions. The intra-assay variability was 4.7%. All measurements were performed in duplicate.

Histological and Immunohistochemical analysis

Pancreas and adipose tissues were placed in 10% neutral buffered formalin (Sigma-Aldrich) for 48 hours and then kept in 70% ethanol. Tissues sections of 5 μm were deparaffinized and dehydrated in a graded series (100% to 70%) of ethanol washes and stained with hematoxylin and eosin (H&E). Langerhans islets were identified and counted using Image J software. Pancreas tissue sections were rinsed in boiled 10 mM citrate buffer solution (pH 6.0) for 20 minutes at room temperature. Sections were quenched for 60 minutes in 1% of 30% hydrogen peroxidase in PBS and washed in TNT wash buffer solution (Tris-buffer 2M, NaCl, Tween 20, dH_2O). A non-specific blocking solution (10% BSA, goat serum, and Triton X-100 BioRad® in PBS) was added and slides were incubated in humidified chamber for 60 minutes at 4°C. Later, sections were incubated with insulin antibody (primary antibody; Cell Signaling Technology®) diluted in blocking solution (1:50) overnight at 4°C. Slides were washed in TNT wash buffer and a secondary antibody (goat anti-rabbit IgG biotin labeled) diluted in blocking solution (1:200) was added for 30 minutes at room temperature and washed again. Next, slides were incubated Streptavidin-HRP diluted in blocking solution (SA-HRP; Perkin Elmer) (1:100) for 30 minutes at room temperature and sections were washed again. Then, Vector® DAB solution, a peroxidase substrate, was added and sections were checked under the microscope until pancreatic insulin expression by β-cells was properly visualized (brown signal). Slides were counterstained with hematoxylin solution Gill n°1 (Sigma-Aldrich).

Dual-energy X-ray absorptiometry (DXA)

Bone mineral density (aBMD), lean mass, and fat mass assessments were performed on each mouse by a PIXImus dual-energy X-ray densitometer (GE Lunar) at the baseline (0), 2 weeks from the baseline (1) and at the endpoint of the study (2). The PIXImus was calibrated daily with a mouse phantom provided by the manufacturer. Mice were placed ventral side down with each limb and tail positioned away from the body. Full-body scans were obtained, and the head was excluded from analyses because of concentrated mineral

content in skull and teeth. X-ray absorptiometry data were processed and analyzed with Lunar PIXImus 2 (version 2.1) software (Motyl et al., 2015).

Micro-computed tomography (μCT)

Micro-architecture of the distal trabecular bone and midshaft cortical bone of the femur, and trabecular bone of the L5 vertebrae, were analyzed by μCT (resolution 10 μm, VivaCT-40, Scanco Medical AG, Bassersdorf, Switzerland). Measurements included femur and vertebrae bone volume/total volume (BV/TV), trabecular number (Tb.N.), trabecular thickness (Tb.Th.), trabecular separation (Tb.Sp.), and connectivity density (Conn.D). Cortical region scans at the midpoint of each femur, with an isotropic pixel size of 21 μm and slice thickness of 21 μm, enabled calculation of average bone area (BA), total cross-sectional area (TA), bone area/total area (BA/TA), and cortical thickness (Ct.Th.). All scans were analyzed using the software of the manufacturer (Scanco Medical AG, version 4.05) (Motyl et al., 2015).

Histomorphometry analysis

Mice were intraperitoneally injected with calcein (20 mg/kg) and demeclocycline (20 mg/kg) on days 9 and 2 before sacrifice, respectively, to determine bone formation rate (de Paula et al., 2011). Left tibias were removed, placed in 70% ethanol and maintained in the dark at room temperature. Tibias were dehydrated with acetone and embedded in methyl methacrylate. Undecalcified 4-μm-thick sections were obtained by microtome and stained with Von Kossa method for showing the mineralized bone. A consecutive section was left unstained for the analysis of fluorescence labeling and was stained with Toluidine Blue for the analysis of osteoblasts, osteoid and adipocytes. Another consecutive section was stained with tartrate-resistant acid phosphatase (TRAP) and counterstained with Toluidine Blue for the analysis of osteoclasts. Bone histomorphometric analysis was performed in the proximal tibia under 200X magnification in a 0.9 mm high × 1.3 mm wide region 200 μm away from the growth plate using OsteoMeasure analyzing software (OsteoMetrics Inc., Decatur, GA, USA). The structural parameters [bone volume (BV/TV), trabecular thickness (Tb.Th), trabecular number (Tb.N) and trabecular separation (Tb.Sp)] were obtained from 3 consecutive sections and the average from these 3 data was assigned as individual data. The structural, dynamic and cellular parameters were calculated and expressed according to the standardized nomenclature (Dempster et al., 2013) as follows: bone volume (BV/TV, %), trabecular thickness (Tb.Th, μm), trabecular number (Tb.N, /mm), trabecular separation (Tb.Sp, μm), mineralizing surface per bone surface (MS/BS, %), mineral apposition rate (MAR, μm/day), bone formation rate per bone surface (BFR/BS, $\mu m^3/\mu m^2$/year), bone formation rate per bone volume (BFR/BV, %/year), bone formation rate per trabecular volume (BFR/TV, %/ year), osteoblast surface (Ob.S/BS, %), osteoblast number per trabecular area (N.Ob/T.Ar, / mm^2), osteoblast number per bone perimeter (N.Ob/B.Pm, / mm), osteoid volume (OV/BV, %), osteoid surface (OS/BS, %), osteoid thickness (O.Th, μm), osteoclast surface (Oc.S/BS, %), osteoclast number per trabecular area (N.Oc/T.Ar, /mm^2) osteoclast number per bone perimeter (N.Oc/B.Pm, /mm), and eroded surface (ES/BS, %), adipocyte volume (Ad.V/TV, %) and number of adipocyte (N.Ad/T.Ar , #/mm^2).

Real-time PCR

Bone marrow was flushed out from the freshly dissected femur and flash frozen in liquid nitrogen separate from the cortical bone. Bone was crushed under liquid nitrogen conditions. Total RNA was prepared using the standard TRIzol (Sigma-Aldrich) method for tissues. cDNA was generated using the High Capacity cDNA Reverse Transcriptase Kit (Applied Biosystems) according to the manufacturer's instructions. mRNA expression analysis was carried out using an iQ SYBR Green Supermix with an iQ5 thermal cycler and detection system (Bio-Rad Laboratories). *Hypoxanthine phosphoribosyltransferase 1* (*Hprt1*) was used as an internal standard control gene for all quantification (Vengellur and LaPres, 2004). Primers were designed and tested to be 95% to 100% efficient by PrimerDesign and primer sequences are listed in Table S2.

Metabolic Cage System

One week before the end of the study, mice from CON-LFD (n=7), CON-HFD (n=7), STZ-LFD (n=6), and STZ-HFD (n=8) groups were placed individually into metabolic cages for 5 days to assess metabolic and behavioral measurements using the Promethion metabolic cage system (Sable Systems International, North Las Vegas, NV) located in the Physiology Core at MMCRI. Data acquisition and instrument control were performed using Meta Screen version 1.7.2.3, and the raw data obtained were processed with ExpeData version 1.5.4 (Sable Systems International, North Las Vegas, NV) using an analysis script detailing all aspects of data transformation (Motyl et al., 2015).

Statistical Analyses

Graphpad Prism® software was used to perform statistical tests. Data are presented as mean ± SEM. Two-way ANOVA with Sidak post hoc test were performed after testing for normal distribution. Where noted, a Pearson correlation test was performed between main outcomes. $\alpha \leq 0.05$ was considered statistically significant.

RESULTS

HFD effects on blood glucose, body composition, insulin and ketones

All mice injected with STZ had high non-fasting glucose levels (>300 mg/dL or 16.7 mmol/L) 12 days after the first injection. Non-fasting glucose levels were still higher in the STZ groups compared to CON groups after 6 weeks of dietary intervention (Figure 1A). However, STZ mice fed with LFD exhibited significantly higher (>600 mg/dL or 33.3 mmol/L) glucose levels compared to those STZ mice fed with HFD (438±70 mg/dL or 24.1±3.9 mmol/L). There was no difference in glucose levels between CON groups fed with LFD or HFD (Figure 1A).

As expected, STZ-LFD mice had significantly lower body weight and body weight gain compared to CON-LFD, and CON-HFD mice gained more weight than CON-LFD mice during the study. Interestingly, STZ-HFD gained body weight throughout the study, whereas STZ-LFD mice did not (Figure 1B). There were no differences in body composition between groups at the baseline and at 2 weeks after baseline (data not shown). At the endpoint, fat mass was significantly reduced in both STZ groups compared to CON groups, and CON-

HFD mice gained a greater amount of fat mass than CON-LFD mice (Figure 1C). However, lean mass was only reduced in STZ-LFD group compared to CON-LFD group. There was no difference in lean mass between STZ-HFD and CON-HFD mice and both CON groups (Figure 1D).

Serum insulin levels were lower in STZ groups compared to Control groups at the endpoint of the study, as expected (Figure 1G). The type of diet consumed (LFD vs. HFD) did not have any impact on serum insulin levels (p=0.66). In order to further characterize the effect of HFD on insulin status in STZ-diabetes, we performed immunohistochemistry (IHC) staining with insulin antibody. IHC analysis demonstrated that STZ mice had lower expression of insulin by pancreatic β-cells compared to the CON groups, which corroborated with serum insulin levels data presented previously. However, there were no overt differences in islets or insulin staining between LFD and HFD STZ groups (Figure 1, E, F and G). To test whether STZ mice were in a state of ketoacidosis, we measured serum β-hydroxybutyrate and found no difference between CON-LFD and STZ-LFD mice (Figure 1H). We did find a significant elevation in β-hydroxybutyrate levels in STZ-HFD mice, consistent with the primary source of fuel being through fat metabolism in these mice.

Effect of Dietary Intervention on Bone Mass and Microarchitecture

In order to determine if the changes in blood glucose and body composition in the STZ groups impacted bone parameters, we addressed BMD by DXA and trabecular and cortical microarchitecture of the femur by microCT (Figure 2). STZ-HFD mice had no temporal reduction in femoral aBMD (Δ value: 0.010± 0.007) during the study while the STZ-LFD mice had (Δ value: −0.001± 0.007) (p=0.002, STZ-LFD vs. STZ-HFD ΔaBMD). At the endpoint, femoral aBMD (and also BMC measurements, not shown) were greater in STZ-HFD than in STZ-LFD mice, although still lower than CON mice (Figure 2B). MicroCT data also corroborated with DXA results showing that STZ-HFD did not lose as much cortical and trabecular bone as those STZ mice consuming LFD. Femoral cortical area fraction (Ct.Ar/Tt.Ar), cortical bone area (Ct.Ar), and cortical thickness (Ct.Th) parameters were significantly lower in the STZ-LFD group compared to the CON-LFD group. Surprisingly, there was no significant difference in these parameters between STZ-HFD and CON-HFD mice (Figure 2, C, D and F). HFD also significantly improved Ct.Ar /Tt.Ar and Ct.Th within the diabetic mouse groups.

Femoral trabecular bone volume fraction (BV/TV), trabecular number (Tb.N), and trabecular connectivity density (Conn.D) parameters were lower in both STZ groups compared to CON mice. However, STZ-HFD mice had a higher femoral trabecular BV/TV, thickness (Tb.Th), Conn.D, and Tb.N compared to STZ-LFD group (Figure 2, H, I, J and L). Structure model index (SMI) was higher in both STZ groups compared to CON groups but SMI was lower in STZ-HFD mice than in STZ-LFD mice (Figure 2K). Furthermore, femoral trabecular separation (Tb.Sp) was higher in the STZ groups compared to CON groups but those STZ mice consuming HFD had lower Tb.Sp compared to the STZ-LFD (0.191 ± 0.003 mm vs. 0.213 ± 0.004 mm, respectively p=0.0002). In the L5 vertebrae, there was a significant main effect of diabetes on BV/TV (p=0.009) but no significant pairwise comparisons between groups. STZ-LFD mice exhibited lower Tb.N and Tb.Th compared to

CON-LFD, but this difference was not present in STZ-HFD mice compared to STZ-LFD mice. Conn.D was also higher in CON-HFD compared to CON-LFD mice and in STZ-HFD group compared to STZ-LFD (Figure 3).

HFD attenuated reduced bone formation in STZ mice

Serum bone formation marker, total procollagen type 1 N-terminal propeptide (P1NP), was lower in STZ-LFD compared to CON-LFD ($p<0.05$) (Figure 4A). There was no difference in P1NP levels between STZ-HFD and CON-HFD groups. However, there was a significant interaction by two-way ANOVA ($p<0.01$) and a trend toward higher P1NP levels in STZ-HFD compared to STZ-LFD mice ($p=0.054$) in the pairwise comparison, suggesting diabetes did not affect bone formation as severely in mice fed a HFD. CTX levels were significantly higher overall in diabetic mice by 2-way ANOVA ($p<0.01$), however, none of the pairwise comparisons reached statistical significance ($p=0.08$ for CON vs. STZ in both the LFD and HFD groups) (Figure 4B). Osteoblast differentiation marker *runt-related transcription factor 2* (*Runx2*) expression was significantly reduced in the STZ-LFD bone compared to CON-LFD bone (Figure 4C), but there was no difference in *bone gamma-carboxyglutamate protein* (*Bglap a.k.a. osteocalcin*) mRNA expression between groups (Figure 4D). *Dentin matrix protein 1* (*Dmp1*) expression was significantly suppressed in STZ-LFD mice compared to CON-LFD, however, it was higher in STZ-HFD mice compared to CON-HFD and STZ-LFD groups (Figure 4E). *Sost* expression was not changed by diabetes or HFD (not shown). Both STZ groups exhibited higher *receptor activator of nuclear factor Kappa-B ligand* (*Rankl*) expression compared to CON groups (Figure 4F). However, *osteoprotegerin (Opg)* mRNA expression was only significantly higher in the STZ-HFD group compared to CON-HFD group (Figure 4G). RANKL/OPG ratio was affected by diabetes and HFD by 2-way ANOVA ($p<0.05$) but none of the pairwise comparisons reached statistical significance (Figure 4H).

Dynamic histomorphometry showed that mineralizing surface (MS) and bone formation rate (BFR/BS) were lower in STZ-LFD group compared to CON-LFD. However, these parameters were not different when comparing CON-HFD mice to STZ-HFD mice (Table 1). Other osteoid and osteoblast parameters were not significantly affected by either STZ or HFD. Additionally, there was a trend toward higher osteoclast number (N.Oc/B.Pm) in STZ-LFD mice compared to CON-LFD ($p=0.08$), but not in HFD fed groups. Furthermore, eroded surface (ES/BS) was significantly higher in STZ-LFD compared to CON-LFD but there was no difference in ES/BS between STZ-HFD and CON-HFD (Table 1).

Marrow adiposity

Dietary intervention and diabetes had a significant interaction effect on marrow adipocytes by two-way ANOVA ($p<0.05$) (Figure 5A–C), however pairwise comparisons did not reach statistical significance. Adipocyte volume (Ad.V/TV) had a tendency to be higher in STZ-LFD mice compared to CON-LFD mice ($p=0.07$) while adipocyte number was not different between groups (Figure 5A–C). Also, there was no difference in *fatty acid binding protein 4* (*Fabp4*) mRNA expression in the marrow between groups (Figure 5D). Conversely, we did observe higher expression of *Adipoq* in STZ-LFD mice compared to CON-LFD, which was not present in the CON-HFD vs. STZ-HFD groups (Figure 5E).

Metabolic and activity outcomes

There was no difference in 24-hour wheel distance meters between groups (Figure 6A). STZ-LFD mice tended to walk less distance meters in 24-hour compared to CON-LFD but it was not significant (p=0.14) (Figure 6B). There was no other significant observation in behavioral parameters such as wheel meters run, wheel speed, % time spent running, walking speed, % time spent walking, % time spent staying still, % time spent sleeping, and hours of sleep (data not shown). Despite no increase in activity, STZ-LFD mice had a higher expenditure energy (EE) compared to CON-LFD and STZ-HFD mice when it was adjusted by lean mass, and CON-HFD mice also had a higher adjusted EE compared to CON-LFD group (Figure 6C). Respiratory quotient (RQ) was different between CON and STZ mice fed with LFD. RQ value was similar between CON-HFD and both STZ groups, which indicated the use of fat as an energy source (Figure 6D).

As expected, STZ-LFD mice had greater water and food intake compared to CON-LFD. However, polydipsia and polyphagia were attenuated in STZ-HFD mice (Figure 7A and 7B). As expected, total calorie intake per body weight was significantly higher in both STZ groups compared to CON groups, but STZ-HFD had lower total calorie intake than STZ-LFD mice (Figure 7C). Concerning macronutrient intake, STZ-LFD mice had a higher carbohydrate intake compared to CON-LFD and STZ-HFD mice (Figure 7D). On the other hand, STZ-HFD group had a greater fat intake than mice from CON-HFD and STZ-LFD groups (Figure 7E). Protein intake was higher in both STZ groups compared to CON groups, and STZ-LFD also had a greater protein consumed than STZ-HFD (Figure 7F).

Correlational analyses between bone and body composition

Body weight had no correlation with femoral aBMD in Control-HFD mice. In contrast, there was a positive correlation between body weight and femoral aBMD in the STZ groups (e.g. STZ-HFD group: r=0.90/p<0.0001; Table 2). Lean mass was strongly correlated with femoral aBMD in all but the CON-LFD groups (e.g. Control-HFD: r =0.80/p=0.003; STZ-LFD: r=0.82/p=0.005; STZ-HFD: r=0.89/p<0.0001), but body fat mass was not correlated with femoral aBMD on any group of the study. We did observe a positive correlation between fat mass and femoral BMC in STZ-HFD (r=0.60/p=0.02). Yet, fat mass had an inverse correlation with femoral BMC in Control-HFD group but it was not significant (r= −0.56/p=0.07). Additionally, there were trends toward a correlation between adipocyte histomorphometry parameters and femoral aBMD and BMC in Control-HFD mice (e.g. Ad.V vs. aBMD: r=0.78/p=0.11 and Ad.V vs. BMC: r=0.85/p=0.06). These correlations were weak in STZ-HFD with no statistical significance. There were no correlations between adipocyte measures and body fat mass (Table 2).

Discussion

We conducted a 6-week dietary intervention to evaluate how nutritional status impacts bone mass in the streptozotocin (STZ)-induced T1DM mouse model. Surprisingly, although HFD feeding generally causes a modest reduction of bone mass, we found that HFD actually attenuated trabecular and cortical bone loss in STZ-diabetic mice. The diabetes-induced reduction of bone formation rate and increase in eroded surface in the LFD mice was not

apparent in the HFD-STZ treated mice. HFD also rescued body weight and lean mass, as well as reduced random fed glucose levels in diabetic mice, indicating that glycaemia and body weight may contribute significantly to diabetic bone outcomes. Moreover, the present study is the first to show a protective effect of HFD rich in MCFA on STZ-induced T1DM bone. Previous studies have reported reduced bone parameters in both T1DM animal models and in human bone biopsies (Botolin and McCabe, 2007; Motyl and McCabe, 2009a; Starup-Linde et al., 2016). T1DM mouse models appear to be more susceptible to trabecular than cortical bone loss, which is consistent with more rapid bone turnover in response to nutritional, hormonal or environmental factors than cortical bone (Botolin and McCabe, 2007). Similarly, young women with T1DM exhibit decreased trabecular bone volume and number (Abdalrahaman et al., 2015). However, in our study we observed both trabecular and cortical bone loss from STZ in the LFD fed mice, which may be related to the duration of the study. In this study, mice were maintained for six weeks after diabetes confirmation, which was two weeks longer than our previous studies examining T1DM bone loss in STZ-treated mice (Botolin and McCabe, 2007; Motyl and McCabe, 2009b; Motyl et al., 2012; Motyl et al., 2011). Histomorphometric parameters demonstrated that bone loss in STZ-LFD group was related to a reduction in bone formation activity and also to an increase in bone resorption, consistent with low serum P1NP levels, down-regulation of *Runx2* and *Dmp1* and up-regulation of *Rankl*. Our findings are similar to other studies showing that bone loss in type 1 diabetic animal models is related to reduction in osteoblast activity and also to a greater osteoclast activity (Coe et al., 2011; Coe et al., 2015; Motyl and McCabe, 2009a; Yee et al., 2016). Tsentidis et al. (Tsentidis et al., 2016) observed high levels of total sRANKL and OPG in T1DM children and adolescents presenting with lower BMD which was associated with increased osteoclast signaling in this population. It is unknown whether bone resorption could be related to diabetes duration and may be an area of interest for future research.

In the present study, STZ mice fed with HFD exhibited a different skeletal outcome, with improvement in femoral aBMD and trabecular and cortical μCT parameters. This is somewhat surprising because previous work had demonstrated reduced trabecular and cortical bone parameters after a HFD (Beamer et al., 2011; Doucette et al., 2015). However, HFD had no effect on trabecular or cortical bone volume or area fraction, respectively, in the control non-diabetic mice in this study. In contrast to our study, most of the studies have adopted a HFD rich in long chain saturated fatty acids (LCFA) that, differently from MCFA, induces a higher body weight gain, a higher endogenous glucose production and a lower glucose rate of disappearance. This could, in addition to duration of the study, explain why we did not observe bone changes with HFD alone (De Vogel-van den Bosch et al., 2011; Omar et al., 2012; Petro et al., 2004). However, we did not find discrepancies between the literature and our study with regards to non-diabetic mice fed the HFD rich in MCFA which exhibited body fat gain but no changes in insulin and glucose levels compared to CON-LFD group (Omar et al., 2012). HFD rich in MCFA need a longer time frame for induction of insulin resistance compared to saturated LFCA HFD. A previous study that had evaluated the same HFD feeding in non-diabetic mice observed increased plasma glucose and insulin levels after 16 weeks of dietary intervention (Surwit et al., 1995). A shorter intervention of 8 weeks only induced fat mass gain without presenting other metabolic changes as we

observed in the present study (Omar et al., 2012). Longer duration studies examining metabolic syndrome-related outcomes in T1DM mice would indeed be interesting and could serve as a natural extension of this work. STZ-LFD mice, however, may not be able to be maintained for longer-term studies as a control since they may begin to exhibit signs of distress which can lead to loss of animals during the study. Any further duration studies may have increased the complexity of interpretations due to increasing severity of diabetes in the STZ-LFD mice, however, in future we plan to perform longer duration studies on STZ-HFD mice alone to determine if protection from diabetes complications persists.

In addition, some studies have investigated the influence of the source of dietary fat on bone metabolism and showed that saturated and polyunsaturated (PUFAs) fat produce different outcomes on skeletal health (Schönfeld and Wojtczak, 2016; St-Onge et al., 2008; Wein et al., 2009). For instance, saturated LCFA intake is associated with reduction in total areal BMC and lumbar spine BMD in non-diabetic animals (Macri et al., 2012) and a decreased femoral BMD in men (Corwin et al., 2006). On the other hand, dietary PUFAs seem to have beneficial effects on bone mass (Bonnet et al., 2014; Farina et al., 2011; Macri et al., 2012). However, most of the studies regarding saturated fat rich in MCFA are focused on its metabolic effects such as reduced body fat mass and enhanced insulin sensitivity (Schönfeld and Wojtczak, 2016; St-Onge et al., 2008; Wein et al., 2009). Only few studies have investigated MCFA role on bone mass and bone remodeling (Doucette et al., 2015; Kim et al., 2014; Nonaka et al., 2016). There has only been one short-term that study has evaluated the effect of HFD rich in MCFA on non-diabetic mouse bone, and it was unchanged after 2 weeks of dietary intervention (Doucette et al., 2015). However, an *in vitro* study demonstrated that capric acid, a MCFA, has inhibitory effects on osteoclastogenesis through suppression of NF-κB and ERK activation and the attenuation of NFATc1 induction (Kim et al., 2014). To our knowledge, no study has specifically addressed lauric acid impact on bone which is the major fatty acid component of coconut oil (Nonaka et al., 2016). Thus, further investigations concerning the impact of MCFAs on bone mass and bone turnover are needed, particularly those that focus on the intestinal microbiome since alterations due to dietary influences in these mice might contribute to changes in bone mass (Zhang et al., 2015).

Bone mass changes in diabetes are likely multifactorial, with hyperglycemia, hypoinsulinemia, nutritional status and presence of diabetes-related complications all contributing to the skeletal pathology (de Paula et al., 2010; Shanbhogue et al., 2016). High glucose levels are associated with advanced glycation end-products (AGEs) that accumulate in the bone organic matrix causing its deterioration (Karim and Bouxsein, 2016). AGEs are thought to alter bone formation activity by inducing osteoblast apoptosis (Alikhani et al., 2007). In diabetic animals, high pentosidine content in the bone tissue was associated with changes in biomechanical properties such as bone stiffness and maximum stress to bone failure, even though there was no reduction in BMD (Saito et al., 2006). Neumann et al. (Neumann et al., 2014) demonstrated that the presence of fractures was associated with elevated pentosidine levels in adult T1DM subjects, independently of BMD. In our study, as expected, multiple doses of STZ caused a decrease in insulin production leading to hyperglycemic conditions. STZ has selective action on β-cells and it does not have any effect on non-β-cells (Eleazu et al., 2013; Lenzen, 2008). The combination of multiple low STZ doses and HFD feeding can also mimic type 2 diabetes metabolic changes. In fact,

literature shows that there is some similarity between early type 1 diabetes and late type 2 diabetes animal models. However, the order of the pathological events is important to better define the diabetic animal model (Skovsø, 2014). In our protocol, β-cells death was induced first with multiple low doses of STZ injections followed by dietary intervention with HFD. Therefore, we produced an early type 1 diabetes animal model (Skovsø, 2014). This model has a similar bone phenotype compared to spontaneous model and it is considered to be a reasonable tool to investigate T1DM bone loss (Motyl and McCabe, 2009a). After 6 weeks of a diet challenge, STZ-HFD mice exhibited lower non-fasting glucose levels compared to LFD feeding group. It is well known that diet composition influences postprandial glucose levels, with the amount and/or type of carbohydrates having the most impact on glycemic control. Dietary fat has also an effect on postprandial hyperglycemia in T1DM subjects (Bell et al., 2015). Even though glycemic control can be improved in diabetic patients by adjusting insulin therapy, diet choice still impacts glycemic control and subsequent complications (Association, 2016). Interestingly, we did not find any rescue effect of HFD feeding on the serum levels of insulin or insulin staining histologically in the pancreas, indicating high glucose, rather than low insulin, was likely playing an important role in the pathophysiology of the skeletal loss. The type of HFD used in the present study had a small proportion of carbohydrates (LFD=73% of Kcal vs. HFD=25.5% of Kcal), which likely contributed to lower glucose levels and ameliorated diabetes symptoms.

In the present study, STZ mice with LFD exhibited classical symptoms of diabetic decompensation including loss of adipose tissue and lean mass after dietary challenge, as seen previously (Motyl and McCabe, 2009a). Conversely, our findings showed that STZ mice fed a HFD had an increase in body weight mostly due to lean mass preservation, as whole body adiposity loss was similar between both STZ groups. A low respiratory quotient (RQ) indicated that all STZ mice were using fat as an energy source (Arch et al., 2006; McClave et al., 2003). However, the difference between the STZ-LFD mice and the STZ-HFD mice was that fat used for fuel was more concentrated in the HFD, while the LFD was a source of fat for fuel, but also contained higher concentrations of carbohydrates. Thus, STZ-LFD mice were significantly polyphagic compared to STZ-HFD mice. Other side effects of polydipsia and polyuria were attenuated with HFD treatment in the STZ mice, indicating slightly better glycemic control. However, these parameters were still higher in STZ-HFD mice compared to CON-HFD. This improvement in the metabolic condition of STZ animals with HFD feeding also led to maintenance of lean mass and, consequently, to bone mass preservation which was not observed in the STZ-LFD group. Insulin therapy would prevent the body fat loss in STZ model. It is important to highlight that insulin treatment would reduce hyperglycemia and other diabetes symptoms and would also increase insulin levels, which is anabolic to bone as described previously (Fulzele et al., 2010). Indeed, past studies have demonstrated that insulin treatment is protective against T1DM-induced bone loss but the mechanism of this still remains unclear due to the multiple outcomes that it modulates (Hough et al., 1981; Verhaeghe et al., 1992). Furthermore, changes in calcitropic hormones are not likely the cause bone loss from STZ-induced diabetes, since others have shown no change in 25-hydroxyvitamin D, parathyroid hormone, or blood or urine calcium levels in this model (Motyl and McCabe, 2009a; Zhang et al., 2016).

Both spontaneous and pharmacologically-induced T1DM mouse models have increased marrow fat content (Botolin and McCabe, 2007). These findings suggest a trend towards adipogenesis in preference to osteogenesis among marrow skeletal progenitor cells. On the contrary, clinical studies have demonstrated no change in total MAT content in vertebral body or femoral bone marrow in T1DM (Slade et al., 2012). In our hands, we observed a significant interaction effect between diabetes and diet on marrow adipocytes. Similarly, we found a trend toward increased adipocyte volume and *Fabp4* expression, as well as a significant increase in *Adipoq* in STZ-LFD mice compared to CON-LFD. These were absent in the HFD mice, suggesting glucose control may be a significant contributor to marrow adipose tissue as described previously in non-diabetic women (de Paula et al., 2015a).

In addition to attenuating hyperglycemia, a possible mechanism for the skeletal protection observed in the STZ-HFD mice might be mediated by an increase in *Opg* expression. Diabetes increased *Opg* expression in the HFD treated mice only, which also attenuated *Rankl/Opg* ratio in HFD fed mice. Studies have demonstrated that fatty acid seems to have a negative role on osteoclast differentiation (Cornish et al., 2008; Philippe et al., 2016) and an increase in *Opg* expression may in part explain bone loss prevention (Philippe et al., 2016). Moreover, mineralization capacity appears to be preserved in STZ-HFD group, which exhibited higher Dmp1 expression, compared to STZ-LFD mice. These findings support STZ-HFD μCT and DXA results found in the present study. Even though there were no differences in histomorphometry bone parameters between diabetic groups, STZ-HFD did not differ from CON-HFD either. In addition, the increase in *Dmp1* and *Opg* expression might suggest that these mice could have bone strength enhanced compared to STZ-LFD group. Improved bone strength and cortical bone biomechanical properties were observed in ovariectomized rats treated with OPG and in transgenic mouse model overexpressing DMP1 (Bhatia et al., 2012; Ominsky et al., 2008). Unfortunately, one limitation of our study was that we did not save bones for testing mechanical and material properties. Our future studies will contain these endpoints and will provide a better understanding of the relationship between bone strength and dietary fat intake in T1DM.

The increase in obesity and overweight appears to be a trend among type 1 diabetic patients and this could lead to a greater susceptibility of developing complications related to excessive body fat accumulation (Conway et al., 2010; da Costa et al., 2016; Liu et al., 2010; Merger et al., 2016; Polsky and Ellis, 2015). On the other hand, our studies suggest that HFD feeding in mice with T1DM may actually improve the skeletal phenotype due to reduced glucose toxicity. Notwithstanding, our animal model may not be the best approach for investigating the impact of obesity in T1DM, as obese/overweight T1DM individuals may not control carbohydrate intake and hyperglycemia in a comparable fashion. Future studies should consider investigating the role of other types of diet on T1DM bone mass, in particular, those diets rich in saturated LCFA which seem to induce a higher fat mass gain and more evident metabolic disorders (De Vogel-van den Bosch et al., 2011; Omar et al., 2012; Petro et al., 2004).

In conclusion, HFD intervention had distinct outcomes in streptozotocin-induced T1DM C57BL/6J male mice. Diabetic mice fed with LFD not only exhibited classical symptoms of diabetes such as polyphagia, polydipsia and hyperglycemia but also bone loss with a marked

reduction in bone formation. But, interestingly, HFD was able to preserve lean mass and attenuate hyperglycemia in streptozotocin-induced T1DM, although it did not produce body fat accumulation in this animal model, as would have been expected. Furthermore, we are the first to show that HFD rich in MCFA was protective against trabecular and cortical bone loss in STZ mice. The type of dietary fat in a HFD might be important for T1DM bone health and will need to be investigated further. The bone-fat interaction in diabetes is multifactorial, with both body weight and glycemic control predominantly contributing. Future studies are necessary to better understand the complexity surrounding the relationship between nutritional status and skeletal remodeling in diabetes, and whether dietary changes may be helpful for bone metabolism without compromising other organ systems.

Supplementary Material

Refer to Web version on PubMed Central for supplementary material.

Acknowledgments

ALC received financial support from FAPESP (2013/09853-6 and 2014/14505-0). FJAP received financial support from CNPq (307901/2014-9) and FAPESP (2014/15864-3). Research reported in this publication was supported by the following National Institutes of Health awards: NIAMS award number AR067858 to KJM, NIDDK award number DK092759 to CJR, NIAMS award number AR068095 to ARG, NIGMS award number GM103392 to Dr. Robert Friesel (MMCRI) and NIGMS award number GM106391 to Dr. Don Wojchowski (MMCRI). The content is solely the responsibility of the authors and does not necessarily represent the official views of the National Institutes of Health. We thank Terry Henderson for technical assistance.

References

Abdalrahaman N, McComb C, Foster JE, McLean J, Lindsay RS, McClure J, McMillan M, Drummond R, Gordon D, McKay GA, Shaikh MG, Perry CG, Ahmed SF. Deficits in Trabecular Bone Microarchitecture in Young Women With Type 1 Diabetes Mellitus. J Bone Miner Res. 2015; 30(8):1386–1393. [PubMed: 25627460]

Alikhani M, Alikhani Z, Boyd C, MacLellan CM, Raptis M, Liu R, Pischon N, Trackman PC, Gerstenfeld L, Graves DT. Advanced glycation end products stimulate osteoblast apoptosis via the MAP kinase and cytosolic apoptotic pathways. Bone. 2007; 40(2):345–353. [PubMed: 17064973]

Arch JR, Hislop D, Wang SJ, Speakman JR. Some mathematical and technical issues in the measurement and interpretation of open-circuit indirect calorimetry in small animals. Int J Obes (Lond). 2006; 30(9):1322–1331. [PubMed: 16801931]

Association AD. Diagnosis and classification of diabetes mellitus. Diabetes Care. 2009; 32(Suppl 1):S62–67. [PubMed: 19118289]

Association AD. 2. Classification and Diagnosis of Diabetes. Diabetes Care. 2016; 39(Suppl 1):S13–22. [PubMed: 26696675]

Basso N, Jia Y, Bellows CG, Heersche JN. The effect of reloading on bone volume, osteoblast number, and osteoprogenitor characteristics: studies in hind limb unloaded rats. Bone. 2005; 37(3):370–378. [PubMed: 16005699]

Beamer WG, Shultz KL, Coombs HF 3rd, DeMambro VE, Reinholdt LG, Ackert-Bicknell CL, Canalis E, Rosen CJ, Donahue LR. BMD regulation on mouse distal chromosome 1, candidate genes, and response to ovariectomy or dietary fat. Journal of bone and mineral research : the official journal of the American Society for Bone and Mineral Research. 2011; 26(1):88–99.

Bell KJ, Smart CE, Steil GM, Brand-Miller JC, King B, Wolpert HA. Impact of fat, protein, and glycemic index on postprandial glucose control in type 1 diabetes: implications for intensive diabetes management in the continuous glucose monitoring era. Diabetes Care. 2015; 38(6):1008–1015. [PubMed: 25998293]

Bhatia A, Albazzaz M, Espinoza Orías AA, Inoue N, Miller LM, Acerbo A, George A, Sumner DR. Overexpression of DMP1 accelerates mineralization and alters cortical bone biomechanical properties in vivo. J Mech Behav Biomed Mater. 2012; 5(1):1–8. [PubMed: 22100074]

Bonnet N, Somm E, Rosen CJ. Diet and gene interactions influence the skeletal response to polyunsaturated fatty acids. Bone. 2014; 68:100–107. [PubMed: 25088402]

Botolin S, McCabe LR. Chronic hyperglycemia modulates osteoblast gene expression through osmotic and non-osmotic pathways. Journal of cellular biochemistry. 2006; 99(2):411–424. [PubMed: 16619259]

Botolin S, McCabe LR. Bone loss and increased bone adiposity in spontaneous and pharmacologically induced diabetic mice. Endocrinology. 2007; 148(1):198–205. [PubMed: 17053023]

Bredella MA, Fazeli PK, Miller KK, Misra M, Torriani M, Thomas BJ, Ghomi RH, Rosen CJ, Klibanski A. Increased bone marrow fat in anorexia nervosa. The Journal of clinical endocrinology and metabolism. 2009; 94(6):2129–2136. [PubMed: 19318450]

Cao JJ. Effects of obesity on bone metabolism. Journal of orthopaedic surgery and research. 2011; 6:30. [PubMed: 21676245]

Coe LM, Irwin R, Lippner D, McCabe LR. The bone marrow microenvironment contributes to type I diabetes induced osteoblast death. J Cell Physiol. 2011; 226(2):477–483. [PubMed: 20677222]

Coe LM, Tekalur SA, Shu Y, Baumann MJ, McCabe LR. Bisphosphonate treatment of type I diabetic mice prevents early bone loss but accentuates suppression of bone formation. Journal of cellular physiology. 2015; 230(8):1944–1953. [PubMed: 25641511]

Conway B, Miller RG, Costacou T, Fried L, Kelsey S, Evans RW, Orchard TJ. Temporal patterns in overweight and obesity in Type 1 diabetes. Diabet Med. 2010; 27(4):398–404. [PubMed: 20536510]

Cornish J, MacGibbon A, Lin JM, Watson M, Callon KE, Tong PC, Dunford JE, van der Does Y, Williams GA, Grey AB, Naot D, Reid IR. Modulation of osteoclastogenesis by fatty acids. Endocrinology. 2008; 149(11):5688–5695. [PubMed: 18617622]

Corwin RL, Hartman TJ, Maczuga SA, Graubard BI. Dietary saturated fat intake is inversely associated with bone density in humans: analysis of NHANES III. J Nutr. 2006; 136(1):159–165. [PubMed: 16365076]

da Costa VM, de Carvalho Padilha P, de Lima GC, Ferreira AA, Luescher JL, Porto L, Peres WA. Overweight among children and adolescent with type I diabetes mellitus: prevalence and associated factors. Diabetol Metab Syndr. 2016; 8:39. [PubMed: 27429649]

de Paula FJ, de Araujo IM, Carvalho AL, Elias J Jr, Salmon CE, Nogueira-Barbosa MH. The Relationship of Fat Distribution and Insulin Resistance with Lumbar Spine Bone Mass in Women. PloS one. 2015a; 10(6):e0129764. [PubMed: 26067489]

de Paula FJ, de Araújo IM, Carvalho AL, Elias J, Salmon CE, Nogueira-Barbosa MH. The Relationship of Fat Distribution and Insulin Resistance with Lumbar Spine Bone Mass in Women. PLoS One. 2015b; 10(6):e0129764. [PubMed: 26067489]

de Paula FJ, Dick-de-Paula I, Bornstein S, Rostama B, Le P, Lotinun S, Baron R, Rosen CJ. VDR haploinsufficiency impacts body composition and skeletal acquisition in a gender-specific manner. Calcif Tissue Int. 2011; 89(3):179–191. [PubMed: 21637996]

de Paula FJ, Horowitz MC, Rosen CJ. Novel insights into the relationship between diabetes and osteoporosis. Diabetes Metab Res Rev. 2010; 26(8):622–630. [PubMed: 20938995]

De Vogel-van den Bosch J, van den Berg SA, Bijland S, Voshol PJ, Havekes LM, Romijn HA, Hoeks J, van Beurden D, Hesselink MK, Schrauwen P, van Dijk KW. High-fat diets rich in medium- versus long-chain fatty acids induce distinct patterns of tissue specific insulin resistance. J Nutr Biochem. 2011; 22(4):366–371. [PubMed: 20655716]

Dempster DW, Compston JE, Drezner MK, Glorieux FH, Kanis JA, Malluche H, Meunier PJ, Ott SM, Recker RR, Parfitt AM. Standardized nomenclature, symbols, and units for bone histomorphometry: a 2012 update of the report of the ASBMR Histomorphometry Nomenclature Committee. J Bone Miner Res. 2013; 28(1):2–17. [PubMed: 23197339]

Devlin MJ, Cloutier AM, Thomas NA, Panus DA, Lotinun S, Pinz I, Baron R, Rosen CJ, Bouxsein ML. Caloric restriction leads to high marrow adiposity and low bone mass in growing mice. J Bone Miner Res. 2010; 25(9):2078–2088. [PubMed: 20229598]

Devlin MJ, Rosen CJ. The bone-fat interface: basic and clinical implications of marrow adiposity. Lancet Diabetes Endocrinol. 2015; 3(2):141–147. [PubMed: 24731667]

Doucette CR, Horowitz MC, Berry R, MacDougald OA, Anunciado-Koza R, Koza RA, Rosen CJ. A High Fat Diet Increases Bone Marrow Adipose Tissue (MAT) But Does Not Alter Trabecular or Cortical Bone Mass in C57BL/6J Mice. Journal of cellular physiology. 2015; 230(9):2032–2037. [PubMed: 25663195]

Eleazu CO, Eleazu KC, Chukwuma S, Essien UN. Review of the mechanism of cell death resulting from streptozotocin challenge in experimental animals, its practical use and potential risk to humans. J Diabetes Metab Disord. 2013; 12(1):60. [PubMed: 24364898]

Farina EK, Kiel DP, Roubenoff R, Schaefer EJ, Cupples LA, Tucker KL. Protective effects of fish intake and interactive effects of long-chain polyunsaturated fatty acid intakes on hip bone mineral density in older adults: the Framingham Osteoporosis Study. Am J Clin Nutr. 2011; 93(5):1142–1151. [PubMed: 21367955]

Fulzele K, Riddle RC, DiGirolamo DJ, Cao X, Wan C, Chen D, Faugere MC, Aja S, Hussain MA, Bruning JC, Clemens TL. Insulin receptor signaling in osteoblasts regulates postnatal bone acquisition and body composition. Cell. 2010; 142(2):309–319. [PubMed: 20655471]

Hough FS, Pierroz DD, Cooper C, Ferrari SL, Bone IC. Diabetes Working G. MECHANISMS IN ENDOCRINOLOGY: Mechanisms and evaluation of bone fragility in type 1 diabetes mellitus. Eur J Endocrinol. 2016; 174(4):R127–138. [PubMed: 26537861]

Hough S, Avioli LV, Teitelbaum SL, Fallon MD. Alkaline phosphatase activity in chronic streptozotocin-induced insulin deficiency in the rat: effect of insulin replacement. Metabolism. 1981; 30(12):1190–1194. [PubMed: 7031417]

Irwin R, Lin HV, Motyl KJ, McCabe LR. Normal bone density obtained in the absence of insulin receptor expression in bone. Endocrinology. 2006; 147(12):5760–5767. [PubMed: 16973725]

Karim L, Bouxsein ML. Effect of type 2 diabetes-related non-enzymatic glycation on bone biomechanical properties. Bone. 2016; 82:21–27. [PubMed: 26211993]

Kawai M, Rosen CJ. The IGF-I regulatory system and its impact on skeletal and energy homeostasis. J Cell Biochem. 2010; 111(1):14–19. [PubMed: 20506515]

Kim HJ, Yoon HJ, Kim SY, Yoon YR. A medium-chain fatty acid, capric acid, inhibits RANKL-induced osteoclast differentiation via the suppression of NF-κB signaling and blocks cytoskeletal organization and survival in mature osteoclasts. Mol Cells. 2014; 37(8):598–604. [PubMed: 25134536]

Komori T. Animal models for osteoporosis. Eur J Pharmacol. 2015; 759:287–294. [PubMed: 25814262]

Lenzen S. The mechanisms of alloxan- and streptozotocin-induced diabetes. Diabetologia. 2008; 51(2):216–226. [PubMed: 18087688]

Liu LL, Lawrence JM, Davis C, Liese AD, Pettitt DJ, Pihoker C, Dabelea D, Hamman R, Waitzfelder B, Kahn HS. Group SfDiYS. Prevalence of overweight and obesity in youth with diabetes in USA: the SEARCH for Diabetes in Youth study. Pediatr Diabetes. 2010; 11(1):4–11. [PubMed: 19473302]

Macri EV, Gonzales Chaves MM, Rodriguez PN, Mandalunis P, Zeni S, Lifshitz F, Friedman SM. High-fat diets affect energy and bone metabolism in growing rats. Eur J Nutr. 2012; 51(4):399–406. [PubMed: 21725629]

McCabe LR. Understanding the pathology and mechanisms of type I diabetic bone loss. Journal of cellular biochemistry. 2007; 102(6):1343–1357. [PubMed: 17975793]

McClave SA, Lowen CC, Kleber MJ, McConnell JW, Jung LY, Goldsmith LJ. Clinical use of the respiratory quotient obtained from indirect calorimetry. JPEN J Parenter Enteral Nutr. 2003; 27(1): 21–26. [PubMed: 12549594]

Merger SR, Kerner W, Stadler M, Zeyfang A, Jehle P, Müller-Korbsch M, Holl RW, Initiative D, mellitus GBCND. Prevalence and comorbidities of double diabetes. Diabetes Res Clin Pract. 2016; 119:48–56. [PubMed: 27449710]

Motyl K, McCabe LR. Streptozotocin, type I diabetes severity and bone. Biol Proced Online. 2009a; 11:296–315. [PubMed: 19495918]

Motyl KJ, DeMambro VE, Barlow D, Olshan D, Nagano K, Baron R, Rosen CJ, Houseknecht KL. Propranolol Attenuates Risperidone-Induced Trabecular Bone Loss in Female Mice. Endocrinology. 2015; 156(7):2374–2383. [PubMed: 25853667]

Motyl KJ, McCabe LR. Leptin treatment prevents type I diabetic marrow adiposity but not bone loss in mice. Journal of cellular physiology. 2009b; 218(2):376–384. [PubMed: 18932203]

Motyl KJ, McCauley LK, McCabe LR. Amelioration of type I diabetes-induced osteoporosis by parathyroid hormone is associated with improved osteoblast survival. Journal of cellular physiology. 2012; 227(4):1326–1334. [PubMed: 21604269]

Motyl KJ, Raetz M, Tekalur SA, Schwartz RC, McCabe LR. CCAAT/enhancer binding protein beta-deficiency enhances type 1 diabetic bone phenotype by increasing marrow adiposity and bone resorption. American journal of physiology Regulatory, integrative and comparative physiology. 2011; 300(5):R1250–1260.

Neumann T, Lodes S, Kastner B, Franke S, Kiehntopf M, Lehmann T, Muller UA, Wolf G, Samann A. High serum pentosidine but not esRAGE is associated with prevalent fractures in type 1 diabetes independent of bone mineral density and glycaemic control. Osteoporosis international : a journal established as result of cooperation between the European Foundation for Osteoporosis and the National Osteoporosis Foundation of the USA. 2014; 25(5):1527–1533.

Nonaka Y, Takagi T, Inai M, Nishimura S, Urashima S, Honda K, Aoyama T, Terada S. Lauric Acid Stimulates Ketone Body Production in the KT-5 Astrocyte Cell Line. J Oleo Sci. 2016; 65(8):693–699. [PubMed: 27430387]

Omar B, Pacini G, Ahrén B. Differential development of glucose intolerance and pancreatic islet adaptation in multiple diet induced obesity models. Nutrients. 2012; 4(10):1367–1381. [PubMed: 23201760]

Ominsky MS, Li X, Asuncion FJ, Barrero M, Warmington KS, Dwyer D, Stolina M, Geng Z, Grisanti M, Tan HL, Corbin T, McCabe J, Simonet WS, Ke HZ, Kostenuik PJ. RANKL inhibition with osteoprotegerin increases bone strength by improving cortical and trabecular bone architecture in ovariectomized rats. J Bone Miner Res. 2008; 23(5):672–682. [PubMed: 18433301]

Paula FJ, Rosen CJ. Obesity, diabetes mellitus and last but not least, osteoporosis. Arq Bras Endocrinol Metabol. 2010; 54(2):150–157. [PubMed: 20485903]

Petro AE, Cotter J, Cooper DA, Peters JC, Surwit SJ, Surwit RS. Fat, carbohydrate, and calories in the development of diabetes and obesity in the C57BL/6J mouse. Metabolism. 2004; 53(4):454–457. [PubMed: 15045691]

Philippe C, Wauquier F, Lyan B, Coxam V, Wittrant Y. GPR40, a free fatty acid receptor, differentially impacts osteoblast behavior depending on differentiation stage and environment. Mol Cell Biochem. 2016; 412(1–2):197–208. [PubMed: 26699911]

Polsky S, Ellis SL. Obesity, insulin resistance, and type 1 diabetes mellitus. Curr Opin Endocrinol Diabetes Obes. 2015; 22(4):277–282. [PubMed: 26087341]

Reid IR. Fat and bone. Arch Biochem Biophys. 2010; 503(1):20–27. [PubMed: 20599663]

Saito M, Fujii K, Mori Y, Marumo K. Role of collagen enzymatic and glycation induced cross-links as a determinant of bone quality in spontaneously diabetic WBN/Kob rats. Osteoporos Int. 2006; 17(10):1514–1523. [PubMed: 16770520]

Schönfeld P, Wojtczak L. Short- and medium-chain fatty acids in energy metabolism: the cellular perspective. J Lipid Res. 2016; 57(6):943–954. [PubMed: 27080715]

Shanbhogue VV, Mitchell DM, Rosen CJ, Bouxsein ML. Type 2 diabetes and the skeleton: new insights into sweet bones. Lancet Diabetes Endocrinol. 2016; 4(2):159–173. [PubMed: 26365605]

Skovsø S. Modeling type 2 diabetes in rats using high fat diet and streptozotocin. J Diabetes Investig. 2014; 5(4):349–358.

Slade JM, Coe LM, Meyer RA, McCabe LR. Human bone marrow adiposity is linked with serum lipid levels not T1-diabetes. Journal of diabetes and its complications. 2012; 26(1):1–9. [PubMed: 22257906]

St-Onge MP, Bosarge A, Goree LL, Darnell B. Medium chain triglyceride oil consumption as part of a weight loss diet does not lead to an adverse metabolic profile when compared to olive oil. J Am Coll Nutr. 2008; 27(5):547–552. [PubMed: 18845704]

Starup-Linde J, Lykkeboe S, Gregersen S, Hauge EM, Langdahl BL, Handberg A, Vestergaard P. Bone structure and predictors of fracture in type 1 and type 2 diabetes. J Clin Endocrinol Metab. 2016:jc20153882.

Surwit RS, Feinglos MN, Rodin J, Sutherland A, Petro AE, Opara EC, Kuhn CM, Rebuffé-Scrive M. Differential effects of fat and sucrose on the development of obesity and diabetes in C57BL/6J and A/J mice. Metabolism. 1995; 44(5):645–651. [PubMed: 7752914]

Tsentidis C, Gourgiotis D, Kossiva L, Doulgeraki A, Marmarinos A, Galli-Tsinopoulou A, Karavanaki K. Higher levels of s-RANKL and osteoprotegerin in children and adolescents with type 1 diabetes mellitus may indicate increased osteoclast signaling and predisposition to lower bone mass: a multivariate cross-sectional analysis. Osteoporos Int. 2016; 27(4):1631–1643. [PubMed: 26588909]

Tuominen JT, Impivaara O, Puukka P, Ronnemaa T. Bone mineral density in patients with type 1 and type 2 diabetes. Diabetes care. 1999; 22(7):1196–1200. [PubMed: 10388989]

Vengellur A, LaPres JJ. The role of hypoxia inducible factor 1alpha in cobalt chloride induced cell death in mouse embryonic fibroblasts. Toxicol Sci. 2004; 82(2):638–646. [PubMed: 15375294]

Verhaeghe J, Suiker AM, Visser WJ, Van Herck E, Van Bree R, Bouillon R. The effects of systemic insulin, insulin-like growth factor-I and growth hormone on bone growth and turnover in spontaneously diabetic BB rats. J Endocrinol. 1992; 134(3):485–492. [PubMed: 1402554]

Wein S, Wolffram S, Schrezenmeir J, Gasperiková D, Klimes I, Seböková E. Medium-chain fatty acids ameliorate insulin resistance caused by high-fat diets in rats. Diabetes Metab Res Rev. 2009; 25(2):185–194. [PubMed: 19219861]

Yee CS, Xie L, Hatsell S, Hum N, Murugesh D, Economides AN, Loots GG, Collette NM. Sclerostin antibody treatment improves fracture outcomes in a Type I diabetic mouse model. Bone. 2016; 82:122–134. [PubMed: 25952969]

Zhang J, Motyl KJ, Irwin R, MacDougald OA, Britton RA, McCabe LR. Loss of Bone and Wnt10b Expression in Male Type 1 Diabetic Mice Is Blocked by the Probiotic Lactobacillus reuteri. Endocrinology. 2015; 156(9):3169–3182. [PubMed: 26135835]

Zhang Y, Wang L, Liu JX, Wang XL, Shi Q, Wang YJ. Involvement of skeletal renin-angiotensin system and kallikrein-kinin system in bone deteriorations of type 1 diabetic mice with estrogen deficiency. Journal of diabetes and its complications. 2016; 30(8):1419–1425. [PubMed: 27614725]

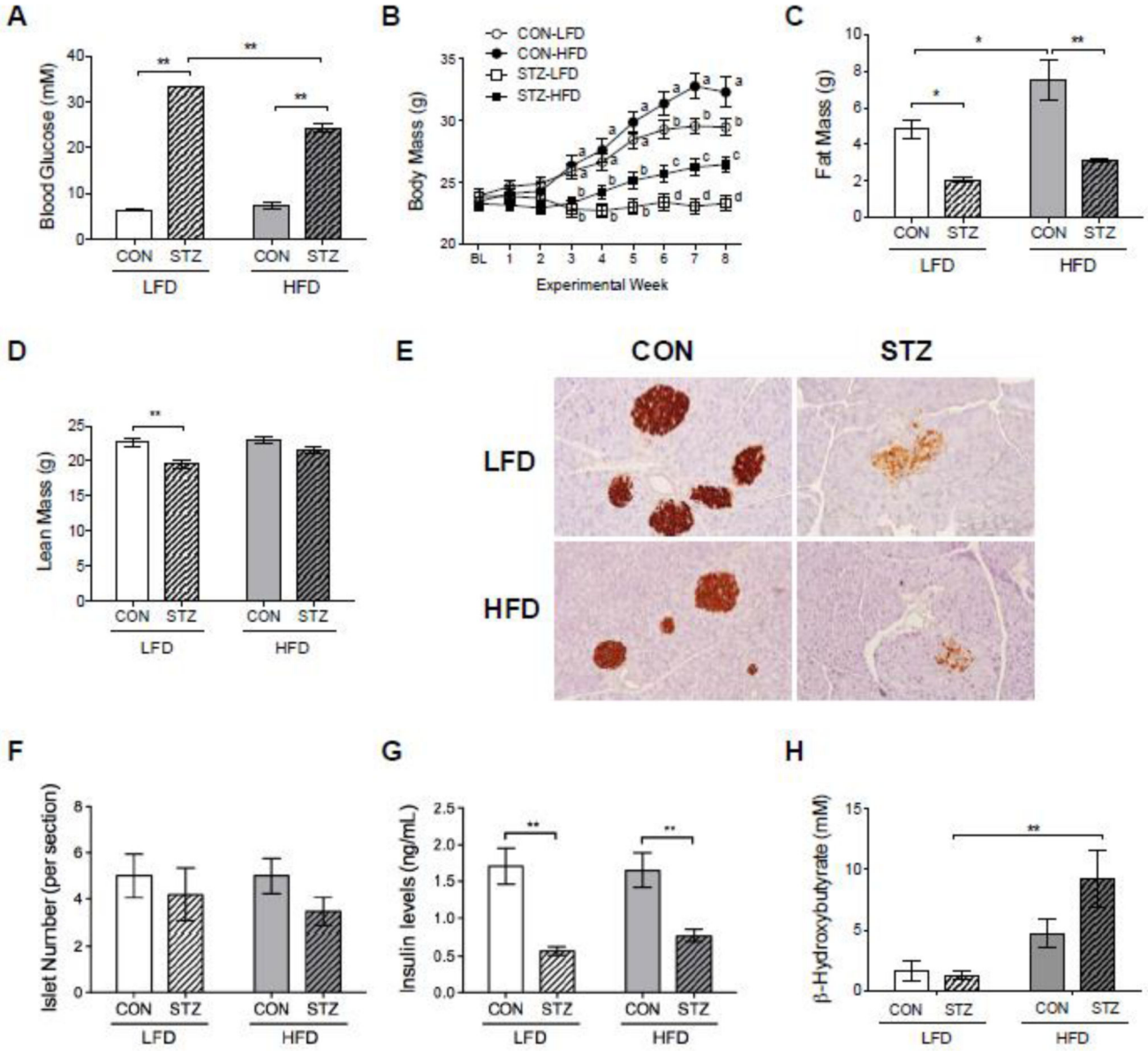

Figure 1.

Effects of HFD on glucose levels, body composition, and insulin. HFD reduced non-fasting blood glucose levels in STZ mice after 6 weeks of dietary intervention (A). Body mass weekly evolution showing that STZ-HFD group had gained more weight than STZ-LFD group (B). Changes in body composition were observed at the endpoint of the study (C and D). Fat mass (C) was significant reduced in STZ mice while lean mass (D) was only lower in STZ-LFD compared to CON-LFD. Detection of insulin production in the pancreatic tissue by immunohistochemistry (IHC) staining (brown signal) (E). Number of Langerhans islets per section of H&E stained pancreatic tissue (F). HFD did not affect insulin levels in diabetic mice (G). Ketone production was addressed with serum β-hydroxybutyrate (H). p-value: *<0.05; **<0.01 by Holm-Sidak post hoc test after a significant 2-way ANOVA. n = 5 to 14.

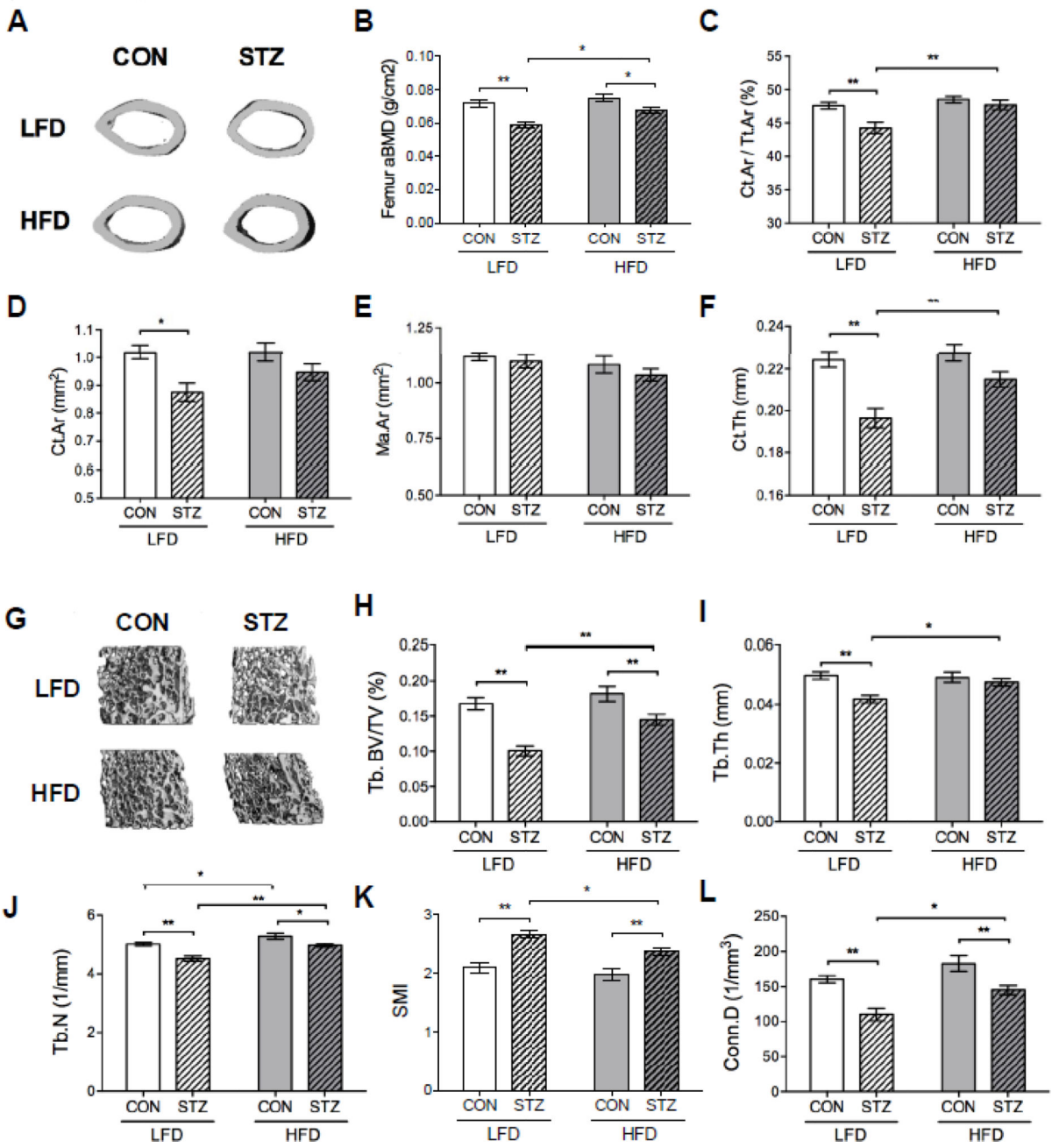

Figure 2.

HFD had a protective effect on bone mass of STZ mice. Representative images of midshaft cortical bone of the femur by μCT analysis (A). Femoral aBMD (g/cm^2) assessed by DXA was preserved in STZ-HFD mice, which was higher compared to STZ-LFD group after 6 weeks of dietary intervention (B). MicroCT parameters corroborated DXA results showing that STZ-HFD had not lost as much trabecular and cortical bone as STZ-LFD mice. Quantitative parameters from μCT of femoral cortical (C, D, E and F) included Ct.Ar/Tt.Ar, Ct.Ar, Ma.Ar and Ct.Th measurements. Representative images of distal trabecular bone of the femur (G) and quantitative parameters of trabecular bone (H, I, J, K and L) by μCT

analysis included BV/TV, Tb.Th, Tb.N, SMI and Conn.D. p-value: *<0.05; **<0.01 by Holm-Sidak post hoc test after a significant 2-way ANOVA. n = 9 to 14.

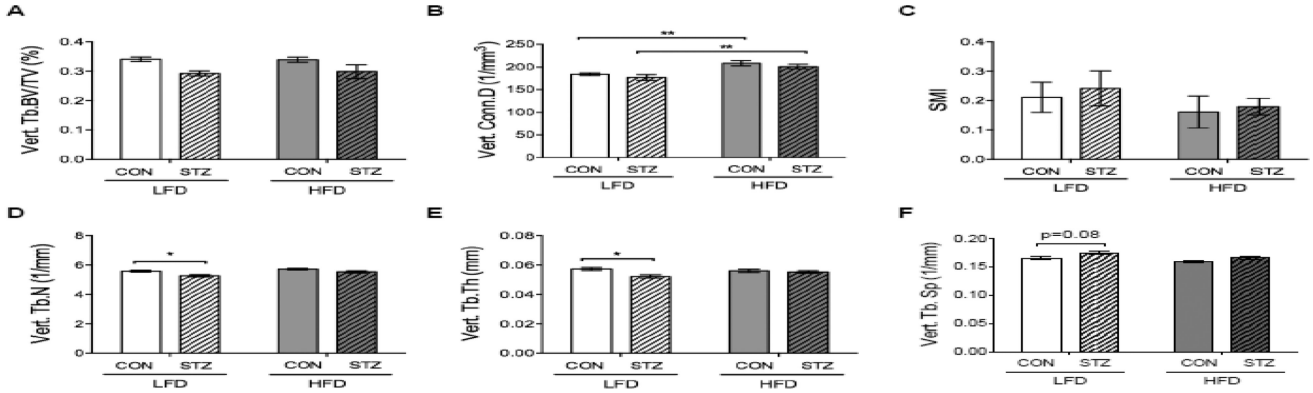

Figure 3.

HFD attenuated STZ-induced effects on vertebral Tb.N and Tb.Th. (A) Tb. BV/TV (STZ main effect $p<0.01$), (B) Conn.D, (C) SMI, (D) Tb.N, (E) Tb.Th and (F) Tb.Sp. was measured in the L5 vertebrae. p-value: *<0.05; **<0.01 by Holm-Sidak post hoc test after a significant 2-way ANOVA. n = 9 to 14.

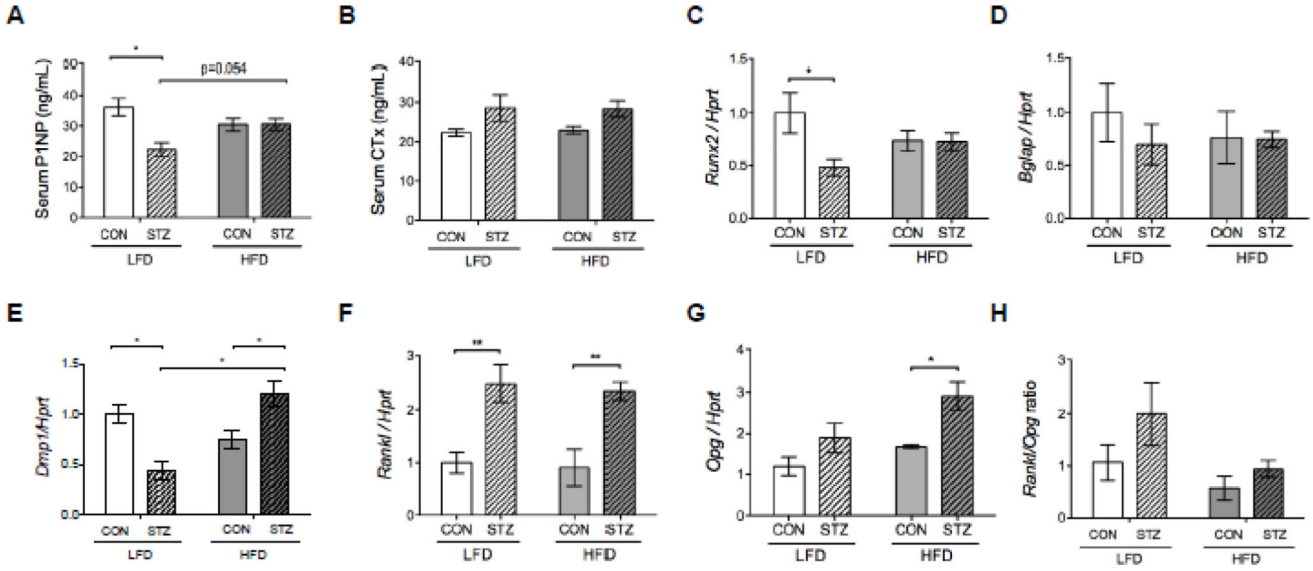

Figure 4.

Serum and mRNA markers of remodeling suggest reduced bone formation in diabetes is attenuated by HFD. Endpoint serum was used to measure P1NP (A) and CTX (B), markers of bone formation and resorption, respectively. Gene expression of (C) *Runx2*, (D) *Bglap*, (E) *Dmp1*, (F) *Rankl* and (G) *Opg* was performed in femurs after marrow had been removed. mRNA expression levels were normalized to the housekeeping gene *Hprt Rankl/Opg* ratio (H) was calculated after normalizing to *Hprt*. p-value: *<0.05; **<0.01 by Holm-Sidak post hoc test after a significant 2-way ANOVA. n = 5 to 11.

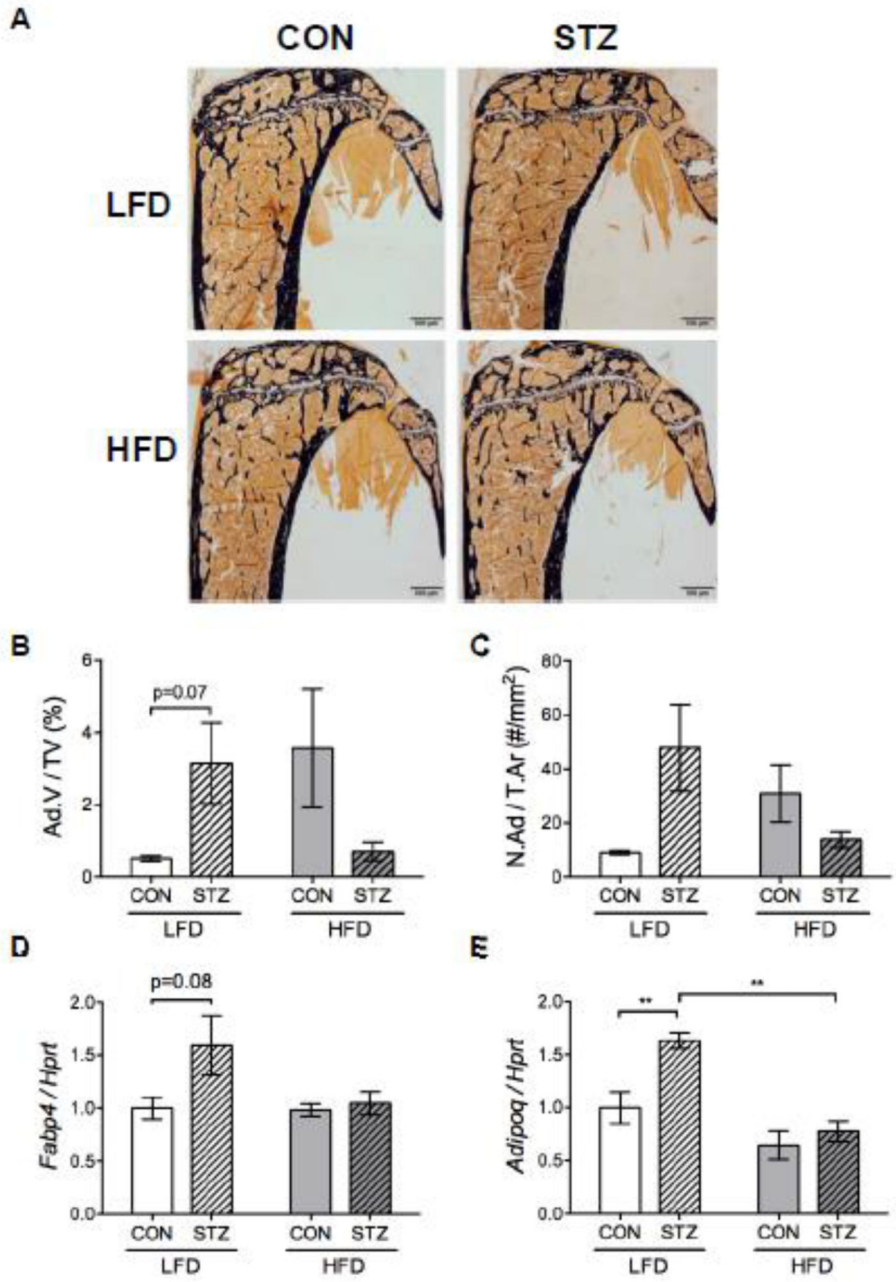

Figure 5.

Diet modulated the effect of diabetes on marrow adipocytes. Representative images from histomorphometric analysis in the proximal tibia, where black stain is mineral (Von Kossa) and adipocytes ghosts are white (A). Adipocyte volume (Ad.V/TV) (B) and number (N.Ad/T.Ar) (C) measurements from the proximal tibia (significant interaction by two-way ANOVA). Gene expression was performed in the frozen marrow tissue content flushed out from the femur at the sacrifice. *Fabp4* (D) and *Adipoq* (E) mRNA expression were normalized to the housekeeping gene *Hprt*. p-value: *<0.05; **<0.01 by Holm-Sidak post hoc test after a significant 2-way ANOVA. n = 6.

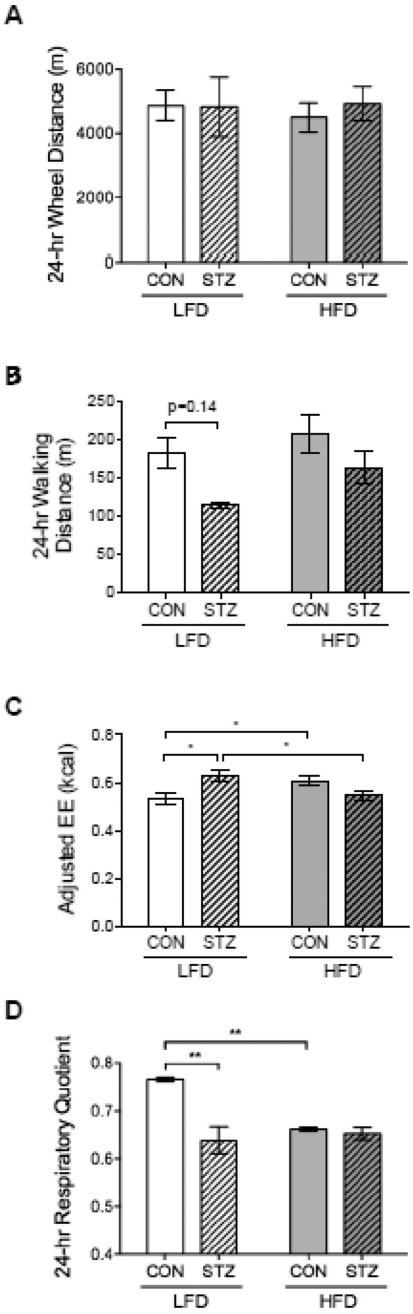

Figure 6.

EE was increased in STZ-LFD mice and RQ value was similar between CON-HFD and both STZ groups indicating fat oxidation. Mice were placed individually into metabolic cages for 5 days, one week before the endpoint. Behavioral measurements included activities as 24-hour wheel distance (A) and walking distance in the cage (B). Metabolic measurements included evaluation of energy expenditure (EE) (C) and 24-hour respiratory quotient (RQ) (D). EE values were adjusted by lean mass. p-value: *<0.05; **<0.01 by Holm-Sidak post hoc test after a significant 2-way ANOVA. n = 6 to 8.

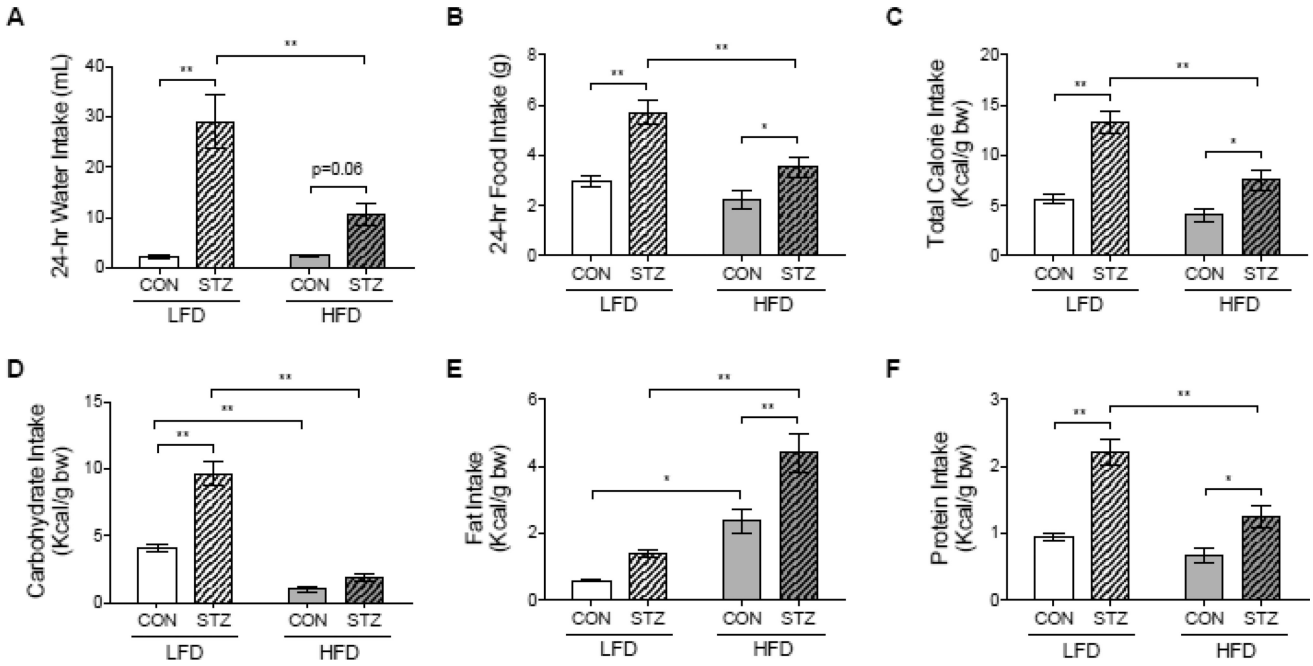

Figure 7.

Diabetes symptoms such as polydipsia and polyphagia were attenuated in STZ-HFD group. Mice were placed individually into metabolic cages one week before the endpoint. 24-hour water (A) and food (B) intake was monitored during for 5 days. Total calorie intake (Kcal/g of body weight) (C), carbohydrate (D), fat (E) and protein (F) intake (Kcal/g of body weight) were calculated based on food intake records. p-value: *<0.05; **<0.01 by Holm-Sidak post hoc test after a significant 2-way ANOVA. n = 6 to 8.

Table 1

Static and dynamic histomorphometry parameters of the proximal tibia from CON and STZ mice fed with LFD or HFD.

	Low Fat Diet		High Fat Diet	
	CON (n=5)	**STZ (n=5)**	**CON (n=5)**	**STZ (n=5)**
OS/BS (%)	9.2 ± 3.1	8.3 ± 4.9	6.1 ± 2.7	6.9 ± 4.0
O.Th (μm)	3.49 ± 0.68	3.45 ± 0.35	3.16 ± 0.63	3.44 ± 0.48
Ob.S/BS (%)	13.1 ± 3.3	9.9 ± 4.4	9.3 ± 5.5	9.7 ± 6.3
N.Ob/B.Pm (/mm)	9.8 ± 2.5	7.6 ± 3.1	6.8 ± 3.8	7.2 ± 4.1
N.Ob/T.Ar (/mm^2)	57.1 ± 9.1	38.1 ± 10.0	43.6 ± 22.4	44.3 ± 35.1
MAR (μm/day)	0.91 ± 0.19	0.88 ± 0.12	0.91 ± 0.13	0.88 ± 0.16
MS/BS (%)	37.5 ± 9.3	18.7 ± 3.8 *	32.1 ± 3.9	25.4 ± 5.3
BFR/BV (%/day)	1.95 ± 0.53	1.20 ± 0.35	1.58 ± 0.37	1.33 ± 0.30
BFR/BS ($\mu m^3/\mu m^2$/day)	0.35 ± 0.12	0.17 ± 0.04 *	0.29 ± 0.05	0.22 ± 0.05
ES/BS (%)	2.87 ± 0.60	5.12 ± 1.37 *	3.61 ± 0.87	4.19 ± 1.65
Oc.S/BS (%)	12.3 ± 2.1	20.6 ± 5.1	13.0 ± 2.5	17.7 ± 6.1
N.Oc/B.Pm (/mm)	4.65 ± 0.75	7.61 ± 1.81	6.09 ± 2.67	7.05 ± 2.41
N.Oc/T.Ar (/mm^2)	27.9 ± 4.3	37.3 ± 7.0	36.6 ± 11.7	40.2 ± 13.8

* $p<0.05$ compared to CON-LFD.

J Cell Physiol. Author manuscript; available in PMC 2019 February 01.

Table 2

Body Composition, Marrow Adipocyte Content and Bone Mass Correlation Matrix from CON and STZ groups.

	Body Weight (g)	Femoral aBMD (g/cm^2)	Femoral aBMC (g)	Lean Mass (g)	Fat Mass (g)	Number of Adipocytes (N.Ad)	Adipocyte Volume (Ad.V)
CON-LFD group							
Body Weight (g)	1						
Femoral aBMD (g/cm^2)	0.51	1					
Femoral aBMC (g)	0.31	0.76*	1				
Lean Mass (g)	0.57	0.58	0.38	1			
Fat Mass (g)	0.66*	0.09	0.005	−0.22	1		
Number of adipocytes (N.Ad)	−0.33	0.35	0.0	−0.87	0.21	1	
Adipocyte Volume (Ad.V)	0.72	0.51	0.43	0.12	0.72	−0.10	1
STZ-LFD group							
Body Weight (g)	1						
Femoral aBMD (g/cm^2)	0.76*	1					
Femoral BMC (g)	0.66	0.87*	1				
Lean Mass (g)	0.94*	0.82*	0.73*	1			
Fat Mass (g)	0.17	0.23	−0.06	0.26	1		
Number of adipocyte (N.Ad)	0.21	−0.50	−0.29	0.22	−0.19	1	
Adipocyte Volume (Ad.V)	0.003	−0.73	−0.57	−0.06	0.01	0.94*	1
CON-HFD group							
Body Weight (g)	1						
Femoral aBMD (g/cm^2)	−0.10	1					
Femoral BMC (g)	−0.26	0.86	1				
Lean Mass (g)	0.11	0.80*	0.76*	1			
Fat Mass (g)	0.93	−0.39	−0.56	−0.25	1		
Number of adipocyte (N.Ad)	−0.37	0.68	0.69	0.86	−0.49	1	
Adipocyte Volume (Ad.V)	−0.57	0.78	0.85	0.87	−0.67	0.97	1
STZ-HFD group							
Body Weight (g)	1						

	Body Weight (g)	Femoral aBMD (g/cm^2)	Femoral aBMC (g)	Lean Mass (g)	Fat Mass (g)	Number of Adipocytes (N.Ad)	Adipocyte Volume (Ad.V)
Femoral aBMD (g/cm^2)	0.90*	1					
Femoral BMC (g)	0.81	0.84	1				
Lean Mass (g)	0.97	0.89*	0.75*	1			
Fat Mass (g)	0.43	0.27	0.60*	0.28	1		
Number of adipocyte (N.Ad)	0.07	−0.02	−0.08	−0.02	0.62	1	
Adipocyte Volume (Ad.V)	−0.10	−0.43	−0.38	−0.19	0.83	0.83	1

* p-value < 0.05.